Probing an intrinsically flavorful ALP via tau-lepton flavor physics

Chuan-Xin Cui,[1,*] Hiroyuki Ishida,[2,†] Shinya Matsuzaki,[1,‡] and Yoshihiro Shigekami[3,§]

[1]*Center for Theoretical Physics and College of Physics, Jilin University, Changchun 130012, China*
[2]*Center for Liberal Arts and Sciences, Toyama Prefectural University, Toyama 939-0398, Japan*
[3]*Tsung-Dao Lee Institute and School of Physics and Astronomy, Shanghai Jiao Tong University, 800 Dongchuan Road, Shanghai 200240, China*

(Received 23 December 2021; accepted 2 May 2022; published 24 May 2022)

Any axionlike particle (ALP) intrinsically possesses flavorful couplings to the standard model (SM) fermions arising as a consequence of the right-handed flavor rotation within the SM. In this paper we discuss this intrinsically flavored ALP, and explore the correlation of a minimal set of the couplings in a view of coherence in flavor physics observables. We focus particularly on the tau-lepton flavor violation (LFV). The ALP is assumed to be tau-philic on a current-eigenstate basis, a la Pecci-Quinn, and is allowed to couple also to muon and electron only in a right-handed specific manner. Several LFV processes are generated including radiative tau decays and also anomalous magnetic moments of electron and muon. We first pay attention to two separated limits: electron scenario with the ALP coupled to tau which mixes only with right-handed electron, and muon scenario as the muonic counterpart of the electron scenario. It turns out that those scenarios are highly constrained by existing experimental limits from the LFV processes and $(g-2)$s, to require a mu or electron-tau flipped feature in the mass eigenbasis when coupled to the ALP. We then examine a hybrid scenario combining the two separated scenarios, and find a fully viable parameter space on the ALP mass-photon coupling plane, which limits the ALP mass to be around (1.7–10) GeV and the ALP decay constant f_a to be (12.8–67.9) GeV. Discrimination of the present ALP from other light LFV particles are also discussed. We find that the same-sign multilepton signal at Belle II is a smoking-gun to probe the present ALP signal, and the polarization asymmetry in LFV radiative τ decay is a punchline, which definitely predicts preference of the right-handed polarization, in sharp contrast to the prediction of the SM plus massive Dirac neutrinos having the highly left-handed preference, and also other light-new physics candidates with the same mass scale as the present ALP. Possible model-building to underlie the intrinsically-flavorful third-generation specific ALP is also briefly addressed.

DOI: 10.1103/PhysRevD.105.095033

I. INTRODUCTION

It is well known that the axion, emergent as a consequence of the Pecci-Quinn (PQ) symmetry breaking, gives a solution for the strong *CP* problem [1–4], which is one of the important issues left in the standard model (SM). The axion generically leaves phenomenological footprints in experiments and astrophysical observations (see Refs. [5,6] as a recent review), which arise associated with presence of the coupling to $U(1)_A$ anomaly, including not only the gluonic, but also the electromagnetic form, and also to the SM-fermion (axial) currents charged under the PQ symmetry. Axions having such phenomenological probes are collectively called axionlike particles (ALPs), and have been keeping the position as one of attractive new physics (NP) candidates, no matter which the ALP may or may not solve the strong *CP* problem.

Of interest is to notice that since the ALP carries an axial charge which it would share with the SM fermions, any ALP possesses intrinsic flavorful couplings to fermions, which arise from the right-handed flavor rotation redundant in the framework of the SM. This is the "minimal flavor violation" (MFV) for the ALP.[1] Plenty of studies on the flavor-physics probes of the ALP have so far been performed. To our best knowledge, however, all those studies have been worked with assuming additional

*cuicx1618@mails.jlu.edu.cn
†ishidah@pu-toyama.ac.jp
‡synya@jlu.edu.cn
§shigekami@sjtu.edu.cn

[1]This MFV is outside the standard definition of the MFV, because the flavorful ALP couplings to fermions also break the family symmetry $U(3)^5$, in addition to the Yukawa sector in the SM.

flavorful couplings beyond the "MFV" framework above: ALP couplings to SM fermions are given as a mixture of the intrinsically flavored part and some underlying ultraviolet (UV) contribution beyond the SM. If one considers some UV physics of the ALP which would not give any flavorful structure, it is still unsure how the intrinsically flavored ALP, constrained by the MFV scheme, could survive or leave a smoking-gun in the flavor physics today, or in the future. This is worth exploring, and is our central motivation in the present work.

In the ballpark of the flavorful-ALP research, the ALP mass range around MeV–GeV has been focused particularly on, because it can be covered by the prospected upcoming experiments, say, the Belle II [7], and can also be desired to explain the current deviation from the SM in anomalous magnetic moment of muon, $(g-2)_\mu$ [8–10],[2] allowing the $a-\mu$ coupling [32–34] and/or the a-photon coupling producing the significant Barr-Zee (BZ) type contribution [35]. It is interesting to also note that this "sweet" mass range coincides with loopholes, yet unconstrained rooms, on the ALP mass-photon coupling space (See, e.g., Refs. [36–40]). Thus, the ALP with the mass ranged around MeV–GeV has been motivated well to be a one promising-NP particle to be probed at the Belle II.

As argued in the recent literature [41], however, it might not be plausible for the ALP to have flavorful couplings which allow the $\mu-e$ conversion [42–44], particularly because of the severe constraint from the muonium-antimuonium oscillation [45]. One way out allowing the ALP to be flavorful may be to apply folklore to the ALP. That is like "*The third-generation is special, and treated differently from the first two.* [46,47]", which has often been motivated in modeling with a flavor symmetry. Since the ALP would be associated with $U(1)$ axial symmetry (or PQ symmetry) of fermions, hence has the type of mass couplings to fermions, the fermion-coupling strengths should generically be aligned to the fermion mass hierarchy, on the basis where the PQ symmetry or the PQ current is defined. Along this criterion, it would be most plausible to assume that the ALP predominantly couples to the third-generation fermions, because they are most massive.

Note also that experimental constraints on lepton flavor violation (LFV) processes involving tau lepton are milder than those for muon decay processes, like $\mu \to e\gamma$, hence the LFV couplings related with tau lepton is allowed to be larger. Tau-LFV processes with ALP have been extensively studied in the literature [48–53]. Therefore, such a third-generation specific ALP with the MFV can potentially be viable in light of searches for tau-LFV processes at the Belle II, within the "sweet," yet unconstrained room (loopholes) above, with keeping high enough sensitivity to $(g-2)_\mu$ as well as $(g-2)_e$.[3]

In this paper, we discuss a third-generation specific and simplified flavorful ALP with the MFV, focusing on the tau-LFV, and explore the intrinsic-flavorful coupling correlations, in light of the Belle II experiment. The ALP is assumed to be tau- and bottom-philic on the base where the "PQ" charge is defined, and can also couple to muon and electron by the MFV arising from the right-handed flavor rotation within the SM. Thus, the ALP couplings to muon and electron are right-handed specific.

We first consider two simplified and separated limits: electron scenario with the ALP coupled to tau which mixes only with right-handed electron, and muon scenario as the muon counterpart of the electron scenario. It turns out that those scenarios are highly constrained by existing experimental limits from the LFV processes and $(g-2)$s, to require a mu or electron-tau flipped feature in the mass eigenbasis when coupled to the ALP.

We then examine a hybrid scenario combining the two separated scenarios, and find a fully viable parameter space on the ALP mass-photon coupling plane, which limits the ALP mass $\sim(1.7-10)$ GeV and the ALP decay constant f_a to be (12.8–67.9) GeV. This ALP can be probed only by measurement of $\tau \to \mu\gamma$ and/or $\tau \to e\gamma$ at Belle II, and cannot be explored by other prospected experiments, including long-lived particle searches. Discrimination of the present ALP from other light LFV particles is also discussed.

We find that the same-sign multilepton signal at Belle II is a smoking-gun to probe the present ALP, and the polarization asymmetry in $\tau \to \mu\gamma$ and/or $\tau \to e\gamma$ is a punchline, which gives a definite prediction of the right-handed polarization due to the MFV, in sharp contrast to the prediction of the SM plus massive Dirac neutrinos having the highly left-handed preference, and also other light-new physics candidates, which are promisingly probed at the Belle II.

This paper is organized as follows. In Sec. II, we start with a generic setup for the ALP couplings, from which the tau-bottom specific ALP with MFV arises, and derive the explicit form of the couplings relevant to the LFV processes as well as $(g-2)_\mu$ and $(g-2)_e$ discussed in Sec. III. Section IV. shows constraints and predictions for two separated scenarios: the electron scenario and muon scenario. In Sec. V, we employ the hybrid scenario and show the viable parameter space projected onto the ALP mass-photon coupling plane. Then, we propose a smoking-gun and a punchline to discriminate the present ALP from other Belle II-targeted NP candidates: that is the polarization

[2]The SM prediction to $(g-2)_\mu$ has so far extensively been studied. See, e.g., Refs. [11–31].

[3]There have been several experimental proposals presented to investigate the loopholes [54–57]. All those proposals are based on parametrically flavorful ALP couplings, in contrast to the present model highly constrained by the MFV criterion.

asymmetry in the radiative tau LFV decay processes. Section VI is devoted to summary of the present paper, and discussion on several issues related to the future prospect along the current work. Possible model-building to underlie the present third-generation specific ALP is also briefly addressed.

II. ALP WITH MFV

We begin by considering the ALP couplings to SM quarks and charged leptons. We assume the CP invariance for the ALP couplings in a current basis on which a PQ-like charge is defined. We consider a minimal set of the ALP couplings described by the following effective quark and lepton mass-matrix terms:

$$\mathcal{L}_{\rm mass}+\mathcal{L}_{aff}=-\bar{q}_i m_q^{ij} q_j-\bar{\ell}_i m_\ell^{ij}\ell_j-i\frac{a}{f_a}\bar{q}_i\gamma_5 C_q^{ij} q_j - i\frac{a}{f_a}\bar{\ell}_i\gamma_5 C_\ell^{ij}\ell_j, \tag{1}$$

where $q=(u,d,s,\cdots,t)^T$ and $\ell=(e,\mu,\tau)^T$ are the quark and lepton fields, respectively; a is represented as the ALP field; f_a is the decay constant of ALP; the sum over the repeated indices are taken into account. We have introduced the ALP-fermion coupling terms as a matrix form, $C_{q,\ell}$, which are taken to be real to keep the CP invariance at this point. For minimality, we assume the coupling matrices to be diagonal in the flavor basis:

$$C_q=\mathrm{diag}\{Q_u m_u, Q_d m_d,\ldots,Q_t m_t\},\quad C_\ell=\mathrm{diag}\{Q_e m_e, Q_\mu m_\mu, Q_\tau m_\tau\}, \tag{2}$$

with the flavor-dependent constants $Q_{q,\ell}$, which can be regarded as the PQ-like charges for the corresponding fermions.

Next, we move on to the mass eigenstate basis of fermions. The criterion of minimality allows the flavor mixing supplied only from the SM sector, i.e., that is the intrinsic flavorful source, what we call the MFV for ALP and is dubbed MFV. Recall the fermion-mass diagonalization in the SM, which is worked out by biunitary (left and right) transformations of the mass matrices. The degree of freedom of the left-handed rotation is completely fixed by the Cabibbo-Kobayashi-Maskawa (CKM) [58,59] and Pontecorvo-Maki-Nakagawa-Sakata (PMNS) angles [60,61], while the right-handed one is unfixed within the SM, to be left as hidden, redundant and unphysical parameters. When the ALP is present and has the chiral couplings to SM fermions, as in Eq. (1), the redundant right-handed rotation actually becomes physical. This is only the flavor-violating source for the ALP within the present MFV framework, and breaks the parity, allowing the ALP to couple to SM fermions, not only in an axial (pseudoscalar) form, but also in a vector (scalar) form.

The rotation matrix of right-handed lepton fields, U_R^ℓ, can be defined in a way similar to the PMNS matrix. We set the CP phase $\delta_{\rm CP}$ to be zero, because the CP violation of lepton sector is not our current concern. The rotation matrix U_R^ℓ is thus parametrized as

$$U_R^\ell=\begin{pmatrix} c_{12}c_{13} & s_{12}c_{13} & s_{13}\\ -s_{12}c_{23}-c_{12}s_{13}s_{23} & c_{12}c_{23}-s_{12}s_{13}s_{23} & c_{13}s_{23}\\ s_{12}s_{23}-c_{12}s_{13}c_{23} & -c_{12}s_{23}-s_{12}s_{13}c_{23} & c_{13}c_{23}\end{pmatrix}, \tag{3}$$

where $c_{ij}=\cos\theta_{ij}$ and $s_{ij}=\sin\theta_{ij}$. By performing this rotation, the Lagrangian terms in Eq. (1) in the mass eigenstate basis are cast into the form:

$$\mathcal{L}'\ni-\bar{q}_i m_{q_i}\delta_{ij}q_j-\bar{\ell}_i m_{\ell_i}\delta_{ij}\ell_j-i\frac{a}{f_a}\bar{q}_i((g_V^q)_{ij}+(g_A^q)_{ij}\gamma_5)q_j-i\frac{a}{f_a}\bar{\ell}_i((g_V^\ell)_{ij}+(g_A^\ell)_{ij}\gamma_5)\ell_j, \tag{4}$$

where the vector and axial couplings are given as

$$g_V^\ell=\frac{C_\ell U_R^\ell-U_R^{\ell\dagger}C_\ell}{2},\qquad g_A^\ell=\frac{C_\ell U_R^\ell+U_R^{\ell\dagger}C_\ell}{2},\qquad g_V^q=0,\qquad g_A^q=C_q. \tag{5}$$

The ALP-photon coupling can be induced through quark and charged-lepton loops at the one-loop order. When the ALP and photons are on-shell, the coupling reads [62]

$$\mathcal{L}_{a\gamma\gamma}=C_{\gamma\gamma}^{\rm eff}\frac{\alpha}{4\pi}\frac{a}{f_a}F_{\mu\nu}\tilde{F}^{\mu\nu}, \tag{6}$$

where

$$C_{\gamma\gamma}^{\rm eff}\equiv\sum_{q_i=u,d,\cdots,t}3(Q_{q_i}^{\rm em})^2\frac{(g_A^q)_{q_iq_i}}{m_{q_i}}B_1\left(\frac{4m_{q_i}^2}{m_a^2}\right)+\sum_{\ell_i=e,\mu,\tau}(Q_{\ell_i}^{\rm em})^2\frac{(g_A^\ell)_{\ell_i\ell_i}}{m_{\ell_i}}B_1\left(\frac{4m_{\ell_i}^2}{m_a^2}\right) \tag{7}$$

where $F_{\mu\nu}$ is the photon field strength; the dual field strength $\tilde{F}^{\mu\nu}$ is defined as $\tilde{F}^{\mu\nu}\equiv\frac{1}{2}\epsilon^{\mu\nu\alpha\beta}F_{\alpha\beta}$, with $\epsilon^{0123}=+1$; α is the fine-structure constant of electromagnetic coupling; $Q_{q_i(\ell_i)}^{\rm em}$ denotes the electric charge (in unit of e) for $i-$ quark ($\ell-$lepton). The loop function $B_1(x)$ is given as

$$B_1(x) = -xf^2(x),$$
$$f(x) = \begin{cases} \sin^{-1}\frac{1}{\sqrt{x}} & \text{for } x \geq 1 \\ \frac{\pi}{2} + \frac{i}{2}\ln\frac{1+\sqrt{1-x}}{1-\sqrt{1-x}} & \text{for } x < 1 \end{cases}. \quad (8)$$

The loop function $B_1(x)$ applied in Refs. [62,63] is $1 - xf^2(x)$, with an extra constant term "1." The difference comes from the model setups.[4] The present ALP model is assumed to have a minimal set of ALP couplings, so that the ALP coupling to photon only arises from one-loop charged fermions, as in Eq. (7). This setup has been realized by requiring a "bare" coupling $C_{\gamma\gamma}^{\rm bare}$ to cancel the electromagnetic $U(1)$ axial anomaly arising due to the anomalous $U(1)_A$ rotation.[5] If those terms had not been made cancelled each other, by going beyond the present minimal setup, we would have the same result on $B_1(x)$ as in Refs. [62,63] with the extra term "1." However, as far as the ALP mass around $\sim\mathcal{O}(\mathrm{GeV})$ is concerned, which is the present target mass range, the numerical evaluation on amplitudes involving this $C_{\gamma\gamma}^{\rm eff}$ coupling would not substantially be altered whether the term "1" is included or not.

It is convenient to further give the relation to the effective ALP-lepton coupling $c_{\ell_i\ell_j}^{\ell}$ adopted in Ref. [62]. Since we focus on the tau-bottom specific ALP, we set $Q_e = Q_\mu = 0$ and $Q_\tau = 1$. Given this benchmark, the effective coupling $c_{\ell_i\ell_j}^{\ell}$ takes the form

$$\text{flavor diagonal: } c_{\tau\tau}^{\ell} = \frac{1}{m_\tau}(g_A^{\ell})_{\tau\tau}, \qquad c_{ee}^{\ell} = c_{\mu\mu}^{\ell} = 0,$$
$$\text{flavor off-diagonal: } c_{\tau\ell_i}^{\ell} = \frac{\sqrt{2}}{m_\tau}\sqrt{|(g_V^{\ell})_{\tau\ell_i}|^2 + |(g_A^{\ell})_{\tau\ell_i}|^2} \quad (\ell_i \neq \tau), \qquad c_{e\mu} = 0. \quad (9)$$

III. RELEVANT LEPTONIC PROCESSES

In this section, we list several leptonic processes, including lepton-flavor conserving and violating physics, such as $(g-2)_e$ and $(g-2)_\mu$, $\ell_i \to \ell_j\gamma$ and $\ell_i \to \ell_j\ell_k\ell_k$. These processes will give constraints on model parameters later, in Sec. IV.

A. Anomalous magnetic moments: $(g-2)_\mu$ and $(g-2)_e$

1. Muon $g-2$

The latest measurement on the anomalous magnetic moment of muon, $a_\mu \equiv (g-2)_\mu/2$, reported by Fermi lab [8], tells us that the combined average with previous result at Brookhaven [9] is 4.2σ deviation from the SM prediction $a_\mu^{\rm SM} = 116591810(43) \times 10^{-11}$ [10] as:

$$\Delta a_\mu \equiv a_\mu^{\rm exp} - a_\mu^{\rm SM} = (2.51 \pm 0.59) \times 10^{-9}. \quad (10)$$

To this discrepancy, the ALP can contribute as the NP term, which can be written as

$$\Delta a_\mu^{\rm NP} = \Delta a_\mu^{\rm BZ} + \Delta a_\mu^{\rm arch}, \quad (11)$$

involving two kinds of diagrams: the BZ and arch loop diagrams as depicted in Fig. 1. The contributions from these two type of diagrams can be evaluated as [37,63,64]

$$\Delta a_\mu^{\rm BZ} = -\frac{m_\mu^2}{16\pi^2 f_a^2}\frac{2\alpha}{\pi}c_{\mu\mu}^{\ell}C_{\gamma\gamma}^{\rm eff}\left[\ln\frac{(4\pi f_a)^2}{m_\mu^2} - h_2(x_\mu)\right], \quad (12)$$

$$\Delta a_\mu^{\rm arch} = \frac{m_\mu^2}{8\pi^2 f_a^2}\sum_{f=e,\mu,\tau}(-(g_V^{\ell})_{\mu f}(g_V^{\ell})_{f\mu}I_{f,1}^{++} + (g_A^{\ell})_{\mu f}(g_A^{\ell})_{f\mu}I_{f,1}^{+-}), \quad (13)$$

where $x_\mu \equiv m_a^2/m_\mu^2$ and the loop functions are

$$h_2(x) \coloneqq 1 + \frac{x^2}{6}\ln x - \frac{x}{3} + \frac{x+2}{3} \times \begin{cases} \sqrt{x(4-x)}\cos^{-1}\frac{\sqrt{x}}{2} & x < 4 \\ -\sqrt{(x-4)x}\ln\frac{\sqrt{x}+\sqrt{x-4}}{2} & x > 4 \end{cases}, \quad (14)$$

$$I_{f,1}^{(\pm)_1(\pm)_2} \coloneqq I_{f,1}[m_{\ell_i}, (\pm)_1 m_{\ell_j}, (\pm)_1 m_{\ell_f}, m_a] = \int dxdydz\delta(1-x-y-z) \times \frac{x(y + (\pm)_1 z\frac{m_{\ell_j}}{m_{\ell_i}}) + (\pm)_2(1-x)\frac{m_{\ell_f}}{m_{\ell_i}}}{-xym_{\ell_i}^2 - xzm_{\ell_j}^2 + xm_a^2 + (1-x)m_{\ell_f}^2}, \quad (15)$$

where m_{ℓ_i} and m_{ℓ_j} correspond to charged-lepton masses in initial and final states for the process, respectively, and m_{ℓ_f} is the charged-lepton mass in the loop.

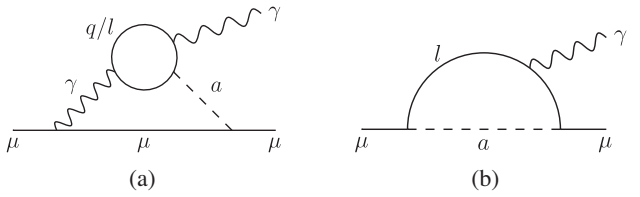

FIG. 1. Illustration of the ALP contributions to Δa_μ: BZ type (Left) and arch type (right). In the BZ type diagram the white blob for the $a-\gamma-\gamma$ vertex is evaluated by the effective coupling $C_{\gamma\gamma}^{\rm eff}$ in Eq. (7). (a) Barr-Zee loop (b) arch loop.

[4]For discussion on this discrepancy, see also Ref. [37].

[5]The most general ALP interactions include the three types: the mass coupling as in Eq. (1), derivative couplings to vector and axial-vector currents, and the "topological-charge" type ($F\tilde{F}$). One of three can be removed by adjusting the axial rotation angle. In this context, the present ALP model has assumed to remove the derivative type of couplings by the axial rotation in the beginning.

In evaluating the BZ diagram in Eq. (12), we have introduced a cutoff scale and replaced it simply by $4\pi f_a$. Presence of the logarithmic divergence is due to the current simplified evaluation of the diagram, in that the $a-\gamma-\gamma$ vertex function is replaced by momentum-independent on-shell-effective coupling $C_{\gamma\gamma}^{\rm eff}$, in such a way that the BZ contribution can be evaluated as an effective one-loop graph. If the BZ diagram were computed exactly at the two-loop level, we would have a finite result as in the literature [65,66]. No matter which evaluation is applied, however, the BZ contribution vanishes in the current tau-specific model with ALP being flavorful via only the right-handed mixing angles, which leads to $c_{\mu\mu}^{l}=0$ from Eq. (9): $\Delta a_\mu^{\rm BZ}=0$.

2. Electron $g-2$

A very recent accurate measurement on the fine-structure constant of the electromagnetic coupling has reported the latest value of the SM prediction to the anomalous magnetic moment of electron, $a_e^{\rm SM}=1159652180.252(95)\times 10^{-12}$ [67]. Comparing to the direct experiment measurement [68], we see about 1.6σ discrepancy:

$$\Delta a_e \equiv a_e^{\rm exp}-a_e^{\rm SM}=(4.8\pm 3.0)\times 10^{-13}. \tag{16}$$

It is worth noting that the two deviations, Δa_e and Δa_μ, have the same signs. Actually, the latest measurement [67] fairly disagrees with the previous results without any clear reason. Therefore, here we also quote the previous value of Δa_e [69,70], the sign of which is opposite compared to Δa_μ:

$$\Delta a_e|_{\rm old}=(-8.7\pm 3.6)\times 10^{-13}. \tag{17}$$

Similarly to Δa_μ in Eq. (11), the ALP contributes to Δa_e as the NP term, which is split into two terms:

$$\Delta a_e^{\rm NP}=\Delta a_e^{\rm BZ}+\Delta a_e^{\rm arch}, \tag{18}$$

where

$$\Delta a_e^{\rm BZ}=-\frac{m_e^2}{16\pi^2 f_a^2}\frac{2\alpha}{\pi}c_{ee}^{\ell}C_{\gamma\gamma}^{\rm eff}\left[\ln\frac{(4\pi f_a)^2}{m_e^2}-h_2(x_e)\right], \tag{19}$$

$$\Delta a_e^{\rm arch}=\frac{m_e^2}{8\pi^2 f_a^2}\sum_{f=e,\mu,\tau}\left(-(g_V^{\ell})_{ef}(g_V^{\ell})_{fe}I_{f,1}^{++}+(g_A^{\ell})_{ef}(g_A^{\ell})_{fe}I_{f,1}^{+-}\right). \tag{20}$$

Again, the present BZ contribution vanishes because $c_{ee}^{l}=0$, from Eq. (9): $\Delta a_e^{\rm BZ}=0$.

B. Radiative LFV: $\ell_i\to\ell_j\gamma$

The branching ratio for $\ell_i\to\ell_j\gamma$ decays process can be evaluated as [32,66]

$$\begin{aligned}{\rm Br}(\ell_i\to\ell_j\gamma)&=\frac{\Gamma(\ell_i\to\ell_j\gamma)}{\Gamma_{\ell_i}},\\ \Gamma(\ell_i\to\ell_j\gamma)&=\frac{\alpha m_{\ell_i}^5(c_{\ell_i\ell_j}^{\ell})^2}{4096\pi^4 f_a^4}\Big|c_{\ell_i\ell_i}^{\ell}g_1(x_{\ell_i})\\ &\quad+\frac{2\alpha}{\pi}\sum\nolimits_{f_i=u,d,\ldots,\mu,\tau}\frac{(g_A^{f})_{f_if_i}}{m_{f_i}}f\left(\frac{m_a^2}{m_{\ell_i}^2},\frac{m_a^2}{m_{f_i}^2}\right)\Big|^2,\end{aligned} \tag{21}$$

where $x_{\ell_i}\equiv m_a^2/m_{\ell_i}^2$ and Γ_{ℓ_i} is the total width of lepton ℓ_i. The loop functions showing up in Eq. (21) are

$$g_1(x)=2\sqrt{4-x}x^{\frac{3}{2}}\cos^{-1}\frac{\sqrt{x}}{2}+1-2x+\frac{3-x}{1-x}x^2\ln x, \tag{22}$$

$$f(u,v)=\int_0^1 dxdydz\frac{ux}{u\bar{x}+uvxyz\bar{z}+vz\bar{z}x^2\bar{y}^2} \tag{23}$$

where $\bar{x}(\bar{y},\bar{z})$ is the shorthand notation for $x(y,z)-1$. Note that in the present ALP model, there are only bottom and τ contributions to the second term in Eq. (21). See Eqs. (33) and (43). In contrast to $\Delta a_\mu^{\rm BZ}$ and $\Delta a_e^{\rm BZ}$ in Eqs. (12) and (19), the overall coupling for the BZ graph contributions is set by the flavor-off diagonal one, $c_{l_il_j}^{l}$, which leads to nonzero contributions [via Eq. (9)] to the radiative LFV processes. However, it will turn out that the BZ terms is actually required to be highly suppressed by phenomenological arguments.

Here we have kept the leading term in expansion with respect to large m_{ℓ_i}, so that only the ℓ_i lepton contribution has been taken into account in evaluating the arch loop, because other terms will either involve flavor changing couplings twice, or be suppressed by the smaller lepton masses, hence are all likely to be subdominant.

C. Purely leptonic LFV: $\ell_i\to\ell_j\ell_k\ell_k$

Other important and stringent constraints would come from purely leptonic LFV processes, like $\ell_i\to\ell_j\ell_k\ell_k$. The mass of ALP is fairly sensitive to those processes: when $m_a<2m_{\ell_k}$ or $m_a>m_{\ell_i}-m_{\ell_j}$, the ALP can only be produced off mass shell, while for $2m_{\ell_k}<m_a<m_{\ell_i}-m_{\ell_j}$, the ALP can be produced at on-shell. For simplicity, we only consider the tree-level contribution from the ALP. The explicit expressions of the branching ratios for those processes are given as follows [63]: for $m_a>m_{\ell_i}-m_{\ell_j}$, we have

$$\Gamma(\ell_i \to \ell_j a^* \to \ell_j \ell_k \ell_k) = \frac{c^2_{\ell_k\ell_k} c^2_{\ell_i\ell_j} m^3_{\ell_i} m^2_{\ell_k}}{256\pi^3 f_a^4} \varphi_0^{jk}(x_{\ell_i}), \quad (24)$$

where

$$\varphi_0^{jj}(x) = -\frac{11}{4} + 4x - \left[\frac{x^2}{2}\ln\frac{2x-1}{x} - 1 + 5x - 4x^2\right] \times \ln\frac{x-1}{x} + \frac{x^2}{2}\left[\mathrm{Li}_2\left(\frac{x-1}{2x-1}\right) - \mathrm{Li}_2\left(\frac{x}{2x-1}\right)\right], \quad (25)$$

$$\varphi_0^{j\neq k}(x) = (3x^2 - 4x + 1)\ln\frac{x-1}{x} + 3x - \frac{5}{2}; \quad (26)$$

for $2m_{\ell_k} < m_a < m_{\ell_i} - m_{\ell_j}$, we have

$$\Gamma(\ell_i \to \ell_j a \to \ell_j \ell_k \ell_k) \approx \Gamma(\ell_i \to \ell_j a)\mathrm{Br}(a \to \ell_k \ell_k) = \tau_a \frac{c^2_{\ell_k\ell_k} c^2_{\ell_i\ell_j} m^3_{\ell_i} m^2_{\ell_k}}{256\pi^2 f_a^4} \times \left(1 - \frac{m_a^2}{m^2_{\ell_i}}\right)^2 \sqrt{m_a^2 - 4m^2_{\ell_k}}, \quad (27)$$

where τ_a denotes the lifetime of ALP.

D. LFV production of on-shell ALP: $l_i \to l_j a$

At tree level, the on-shell ALP can be generated through the decay process $\ell_i \to \ell_j a$ and its partial width is computed as [63]

$$\Gamma(\ell_i \to \ell_j a) = \frac{m^3_{\ell_i}}{32\pi}\left(1 - \frac{m_a^2}{m^2_{\ell_i}}\right)^2 \frac{c^2_{\ell_i\ell_j}}{f_a^2}. \quad (28)$$

E. Experimental limits

In Table I, we give a summary of the currently available experimental bounds and future prospected limits on the tau-LFV processes.

TABLE I. Current and future prospected limits on the relevant tau-LFV processes.

LFV process	Experiment limit with 90% CL	Future prospect
$\tau \to e\gamma$	3.3×10^{-8} [71]	3×10^{-9} [56]
$\tau \to \mu\gamma$	4.4×10^{-8} [71]	10^{-9} [72]
$\tau \to 3e$	2.7×10^{-8} [71]	5×10^{-10} [56]
$\tau \to 3\mu$	2.1×10^{-8} [71]	4×10^{-10} [56]
$\tau \to e\mu^+\mu^-$	2.7×10^{-8} [71]	6×10^{-10} [56]
$\tau \to \mu e^+ e^-$	1.8×10^{-8} [71]	3×10^{-10} [56]
$\tau \to e + \mathrm{inv}$	$\approx 2.7 \times 10^{-3}$ [73]	…
$\tau \to \mu + \mathrm{inv}$	$\approx 5 \times 10^{-3}$ [73]	…

IV. TWO SCENARIOS FOR BOTTOM-TAU SPECIFIC MODEL

In this section, we investigate two separated scenarios for the third-generation specific model relevant to the tau-lepton flavor physics, as well as Δa_e and/or Δa_μ. We employ the two separated scenarios: the electron scenario and muon scenario. For the electron scenario, we turn on only θ_{13}, which connects the tau and electron flavor physics. While for the muon scenario, only θ_{23} is taken to be nonzero, to allow tau and muon flavor physics to be correlated. We maximize the ALP coupling to bottom quark, by simply assuming no flavor mixing with the ALP in the quark sector, i.e., $\theta_q = 0$. The setup for the lepton sector in these two scenarios is summarized in Table II.

A. Electron scenario

In this scenario, there are only two nonzero couplings to SM fermions left:

$$c_{\tau\tau} = \cos\theta_{13}, \qquad c_{e\tau} = \sin\theta_{13}. \quad (29)$$

Then the ALP-photon coupling in Eq. (7) is now simplified to

$$C_{\gamma\gamma}^{\mathrm{eff}} = \frac{1}{3}B_1\left(\frac{4m_b^2}{m_a^2}\right) + \cos\theta_{13} B_1\left(\frac{4m_\tau^2}{m_a^2}\right). \quad (30)$$

Note that $C_{\gamma\gamma}^{\mathrm{eff}}$ does not simply scale with θ_{13} because it involves the bottom-quark loop contribution, hence the sign of $\cos\theta_{13}$ becomes relevant, and θ_{13} is allowed to take the values in the first and the second quadrants, i.e., $\theta_{13} \in [0, \pi]$.

Similarly, we can simplify Δa_e^{NP} in Eq. (18) with Eqs. (19) and (20), $\tau \to e\gamma$ in Eq. (21) with Eq. (23), and $\tau \to ea$ in Eq. (28), to get

$$\Delta a_e^{\mathrm{NP}} = \frac{\sin^2\theta_{13}}{f_a^2} F_1(m_a), \quad (31)$$

$$Br[\tau \to ea] = \frac{\sin^2\theta_{13}}{f_a^2} F_2(m_a), \quad (32)$$

$$Br[\tau \to e\gamma] = \frac{\sin^2\theta_{13}}{f_a^4} F_3(m_a)\left|\cos\theta_{13} g_1\left(\frac{m_a^2}{m_\tau^2}\right) + \frac{2\alpha}{\pi}\left[f\left(\frac{m_a^2}{m_\tau^2}, \frac{m_a^2}{m_b^2}\right) + \cos\theta_{13} f\left(\frac{m_a^2}{m_\tau^2}, \frac{m_a^2}{m_\tau^2}\right)\right]\right|^2, \quad (33)$$

where $F_1(m_a)$, $F_2(m_a)$, and $F_3(m_a)$ are defined as

$$F_1(m_a) = \frac{m_e^2 m_\tau^2}{32\pi^2}(I_{f,1}^{++} + I_{f,1}^{+-}), \quad (34)$$

TABLE II. The electron and muon scenarios with the corresponding parameter setup in the lepton sector, and the associated LFV processes as well as the lepton $(g-2)$s.

Third-generation specific model with $Q_\tau = Q_b = 1$, other $Q_f = 0$		
Scenario	Parameter setup	Nonzero leptonic processes
Electron scenario	$\theta_{13} \neq 0$, $\theta_{23} = \theta_{12} = 0$	Δa_e, $\tau \to e\gamma$, $\tau \to e + \text{inv}$
Muon scenario	$\theta_{23} \neq 0$, $\theta_{13} = \theta_{12} = 0$	Δa_μ, $\tau \to \mu\gamma$, $\tau \to \mu + \text{inv}$

$$F_2(m_a) = \tau_\tau \frac{m_\tau^5}{32\pi}\left(1 - \frac{m_a^2}{m_\tau^2}\right)^2 \frac{1}{m_\tau^2}, \tag{35}$$

$$F_3(m_a) = \tau_\tau \frac{\alpha m_\tau^5}{4096\pi^4}. \tag{36}$$

It is interesting to note that the present ALP generically gives a positive contribution to Δa_e, because $F_1(m_a)$ is positive definite.

In Fig. 2 we show the numerical result on Δa_e (left panel) and $Br[\tau \to e\gamma]$ (right panel), for $m_a = 2$ GeV, with f_a varied. As seen from the figure, $\tau \to e\gamma$ process tends to be predicted to be too large ($\mathcal{O}(1)$) to survive the current experiment limit ($\mathcal{O}(10^{-8})$ as in Table I). There exists a destructive cancellation between the arch and BZ diagrams, where the dominant contribution comes from the τ arch loop. Thus $Br[\tau \to e\gamma]$ approximately scales with $\sin^2\theta_{13}\cos^2\theta_{13}$. Hence, to realize small enough $Br[\tau \to e\gamma]$ while still keeping sizable deviation of Δa_e, θ_{13} should be fine-tuned to around $\pi/2$, close to the exact cancellation between the τ arch loop and the BZ contributions. Below we give the precise value of the allowed region for θ_{13} when $m_a = 2$ GeV:

$$f_a = 10.8\ \text{GeV}, \quad \theta_{13} \simeq 1.55132\text{–}1.55152, \quad \text{Br}[\tau \to e\gamma] = (0\text{–}3.3) \times 10^{-8} \tag{37}$$

$$f_a = 14\ \text{GeV}, \quad \theta_{13} \simeq 1.54966\text{–}1.55001, \quad \text{Br}[\tau \to e\gamma] = (0\text{–}3.3) \times 10^{-8} \tag{38}$$

$$f_a = 28\ \text{GeV}, \quad \theta_{13} \simeq 1.54482\text{–}1.54622, \quad \text{Br}[\tau \to e\gamma] = (0\text{–}3.3) \times 10^{-8} \tag{39}$$

As evident from Eq. (34), the ALP contribution to Δa_e is necessarily positive. For Δa_e to stay in the region within the 2σ deviation, the decay constant f_a is thus constrained to be larger than 10.8 GeV when $m_a = 2$ GeV. If we adopt the previous value of Δa_e, $\Delta a_e|_{\text{old}} = (-8.7 \pm 7.2) \times 10^{-13}$ in Eq. (17), then the present ALP cannot account for Δa_e, rather, would be ruled out.

The ALP gets further constraints coming from $\tau \to ea$, where the on-shell ALP is generated through the tau decay process. The straightforward numerical calculation shows

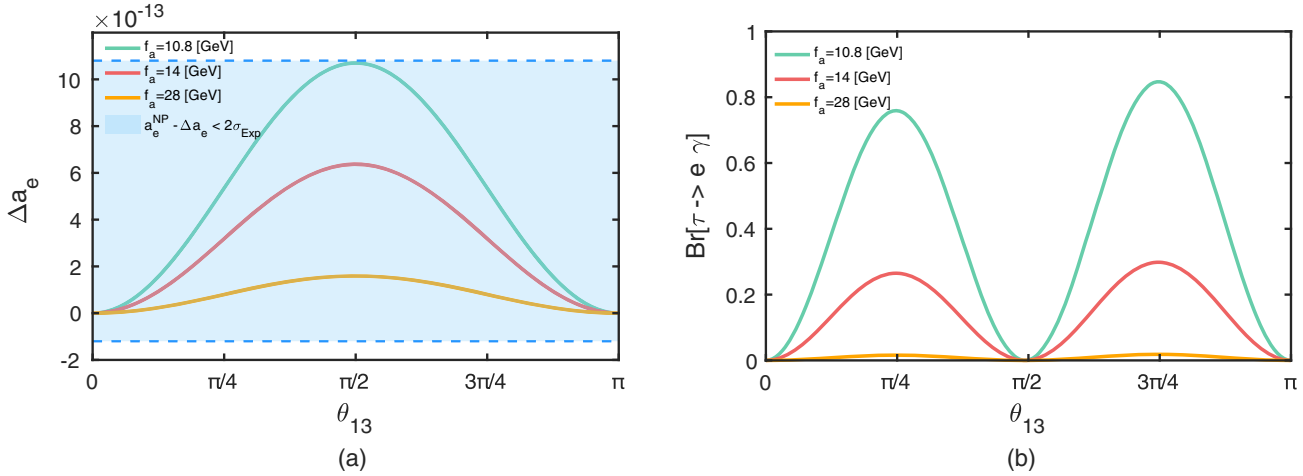

FIG. 2. (Electron scenario): θ_{13} dependence of Δa_e (left panel) and $Br[\tau \to e\gamma]$ (right panel). In the left panel, the blue band stands for the currently allowed region within the 2σ deviation read off from Eq. (16). The ALP mass m_a has been set to 2 GeV in the plots. (a) Δa_e (b) $\tau \to e\gamma$.

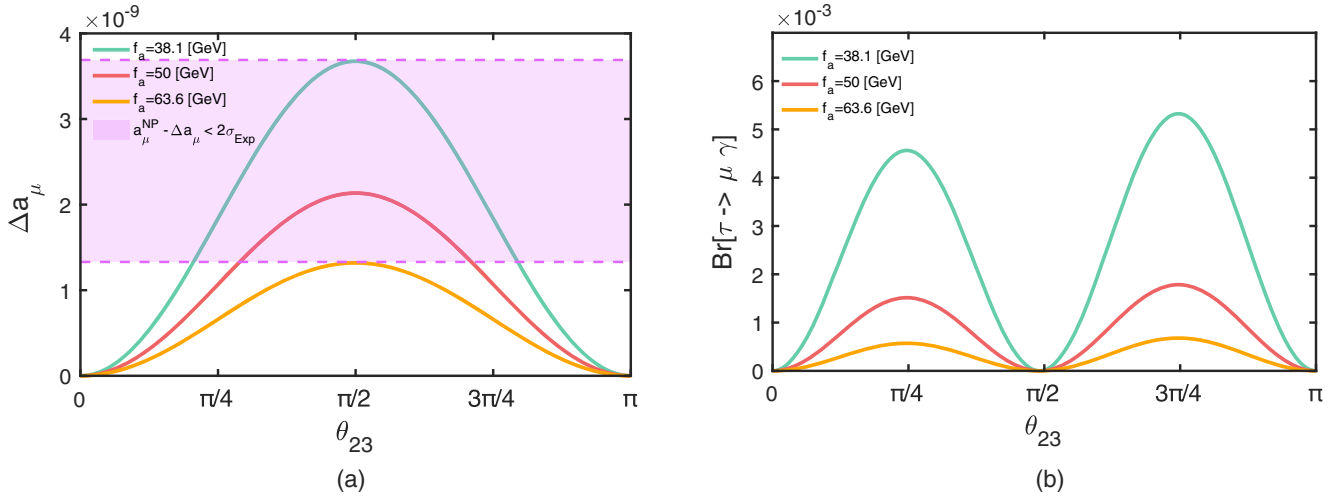

FIG. 3. (Muon scenario): θ_{23} dependence on Δa_μ (left panel) and $Br[\tau \to \mu\gamma]$ (right panel). In the left panel, the purple band stands for the 2σ allowed range read off from Eq. (10). The ALP mass m_a has been set to 2 GeV in two figures. (a) Δa_μ (b) $\tau \to \mu\gamma$.

that $F_2(m_a)/f_a^2$ in Eq. (32) gives too big branching ratio value compared to the experiment constraint except for θ_{13} taking the value extremely close to 0 or π. However, $\theta_{13} \sim 0$ or π would yield $\Delta a_e \ll 10^{-13}$, which would still be consistent with current measurement of Δa_e within the 2σ error in Eq. (16), though being trivial in a sense of no LFV. Nevertheless, we shall simply exclude the possibility of this case with the on-shell ALP production through $\tau \to ea$,[6] such that the present ALP mass is constrained as $m_a > m_\tau - m_e \simeq 1.78$ GeV.

B. Muon scenario

In the muon scenario with only nonzero θ_{23}, we have two nonzero couplings to SM leptons:

$$c_{\tau\tau} = \cos\theta_{23}, \qquad c_{\mu\tau} = \sin\theta_{23}. \tag{40}$$

Then all the analytic formulas for the ALP-photon coupling and relevant LFV amplitudes take essentially the same form as those in the electron scenario, just by replacing θ_{13} with θ_{23} in Eqs. (30)–(33) and substituting m_e^2 with m_μ^2 in Eq. (34):

$$\Delta a_\mu^{\rm NP} = \frac{\sin^2\theta_{23}}{f_a^2} F_1(m_a), \tag{41}$$

$$Br[\tau \to \mu a] = \frac{\sin^2\theta_{23}}{f_a^2} F_2(m_a), \tag{42}$$

$$Br[\tau \to \mu\gamma] = \frac{\sin^2\theta_{23}}{f_a^4} F_3(m_a) \left| \cos\theta_{23} g_1\left(\frac{m_a^2}{m_\tau^2}\right) + \frac{2\alpha}{\pi}\left[f\left(\frac{m_a^2}{m_\tau^2}, \frac{m_a^2}{m_b^2}\right) + \cos\theta_{23} f\left(\frac{m_a^2}{m_\tau^2}, \frac{m_a^2}{m_\tau^2}\right)\right]\right|^2. \tag{43}$$

The numerical results on Δa_μ and $Br[\tau \to \mu\gamma]$ are presented in Fig. 3, for $m_a = 2$ GeV with f_a varied, in a way similar to the electron scenario (Fig. 2). The current $\tau \to \mu\gamma$ limit only allows tiny window for θ_{23}, where θ_{23} should be bounded around $\pi/2$ to cause the almost exact cancellation between the τ arch loop and the BZ term contributions [See Eq. (43)]. Therefore, with $\theta_{23} \simeq \pi/2$, the decay constant f_a is constrained and allowed to vary only in a small range, 38.1 GeV–63.6 GeV, to yield Δa_μ within the 2σ deviation [See Eq. (41)]. Similarly to the electron scenario, the on-shell ALP prodution via $\tau \to \mu a$ is rule out, and this gives the lower bound on the ALP mass, $m_a \gtrsim 1.67$ GeV. Below we also give the precise θ_{23} region when $m_a = 2$ GeV:

$$f_a = 38.1 \text{ GeV}, \qquad \theta_{23} \simeq 1.54205\text{–}1.54506, \quad \mathrm{Br}[\tau \to \mu\gamma] = (0\text{–}4.4) \times 10^{-8} \tag{44}$$

$$f_a = 50 \text{ GeV}, \qquad \theta_{23} \simeq 1.53923\text{–}1.54442, \quad \mathrm{Br}[\tau \to \mu\gamma] = (0\text{–}4.4) \times 10^{-8} \tag{45}$$

$$f_a = 63.6 \text{ GeV}, \qquad \theta_{23} \simeq 1.53605\text{–}1.54447, \quad \mathrm{Br}[\tau \to \mu\gamma] = (0\text{–}4.4) \times 10^{-8} \tag{46}$$

[6]There is another important limit on tau-LFV decay processes, like $\tau \to e + \text{inv}$. However, in the present ALP model, this process does not give further constraint on the model parameters when we consider the $\tau \to ea$ process, since the overall factor $F_2(m_a)/f_a^2$ in Eq. (32) is always too big to be survived under experiment constraint. Therefore, the present model will always be excluded once we allow the on-shell ALP production, which is irrespective to whether the ALP decays inside, or outside the detector.

Thus, both two scenarios that we have discussed above are constrained to have the flavorful ALP coupling with $\theta_{13} \simeq \pi/2$ or $\theta_{23} \simeq \pi/2$. It would be intriguing to note that this indicates the preference of a mu or electron-tau flipped feature in the mass eigenbasis when coupled to the ALP. In the next section, we will go beyond these specific scenarios, and employ a hybrid scenario by turning on both θ_{13} and θ_{23}, and will find the surviving parameter space under all the existing relevant constraints. Of particular interest is in a hybrid scenario that the currently measured size of deviation in both Δa_e and Δa_μ may be explained simultaneously.

V. A HYBRID SCENARIO

With both nonzero θ_{13} and θ_{23}, we find the nonzero ALP couplings to SM charged leptons:

$$c_{\tau\tau} = \cos\theta_{23}\cos\theta_{13},$$
$$c_{\mu\tau} = \sin\theta_{23},$$
$$c_{e\tau} = \cos\theta_{23}\sin\theta_{13}. \tag{47}$$

In this section, we focus mainly on the ALP mass within the promising Belle II reach with the high sensitivity (100 MeV $\lesssim m_a \lesssim$ 10 GeV), and search the surviving ALP-photon coupling space over existing and upcoming experimental limits (Part A). Then we propose a smoking-gun and a punchline of the ALP, where in particular the latter is the photon polarization asymmetry λ_γ, clearly distinguishable from other NP candidate with the same mass scale, which can also account for the current deviations in Δa_e and Δa_μ (Part B). Finally, we make precise comparison of the ALP with other NP candidates in a sense of phenomenology (Part C).

A. Experimental constraints on ALP-photon coupling within Belle II reach

In Fig. 4, we show the exclusion plot for the ALP parameter space spanned by $(m_a, g_{a\gamma\gamma})$, where

$$g_{a\gamma\gamma} \equiv \frac{\alpha|C_{\gamma\gamma}^{\rm eff}|}{\pi f_a}. \tag{48}$$

The existing experimental limits include $e^+e^- \to 3\gamma$ at Belle II [7], a photon-beam experiment [74], and heavy-ion collisions [75]; electron beam dump experiments [38]; and SN 1987A [76]. We have also incorporated the SHiP prospect [77], the future Belle II prospects at 20 fb^{-1} and 50 ab^{-1} [38], and also the prospected Belle II limit on the same-sign multileptons signal at 50 ab^{-1} [78]. We find the following features:

(i) Both $\tau \to \mu\gamma$ and $\tau \to e\gamma$ processes require the almost exact cancellation between the τ arch loop and the BZ contributions, as in the case of the muon and electron scenarios. Hence θ_{23} is severely constrained to be around $\pi/2$, so that the ALP photon coupling $C_{\gamma\gamma}^{\rm eff}$ is dominated by bottom quark loop, $C_{\gamma\gamma}^{\rm eff} \sim \frac{1}{3}B_1(\frac{4m_b^2}{m_a^2})$.[7] Note that this almost complete cancellation condition is not sensitive to $Br[\tau \to \mu\gamma]$, nor $Br[\tau \to e\gamma]$. If $\tau \to \mu(e)\gamma$ is observed at Belle II with the prospected branching ratio of $\mathcal{O}(10^{-9})$, it can still be consistent with the present ALP.

(ii) f_a is constrained and allowed to vary in a narrow range,

$$f_a \simeq (12.7\text{–}93.3)\ \text{GeV}, \quad \text{for } m_a = (0.1\text{–}10)\ \text{GeV}. \tag{49}$$

In such scope of f_a, the predicted deviation of Δa_e is on the order of magnitude of $\mathcal{O}(10^{-14})$, which is too small that the current experiment limit on Δa_e cannot give any constraint on θ_{13}. However, the

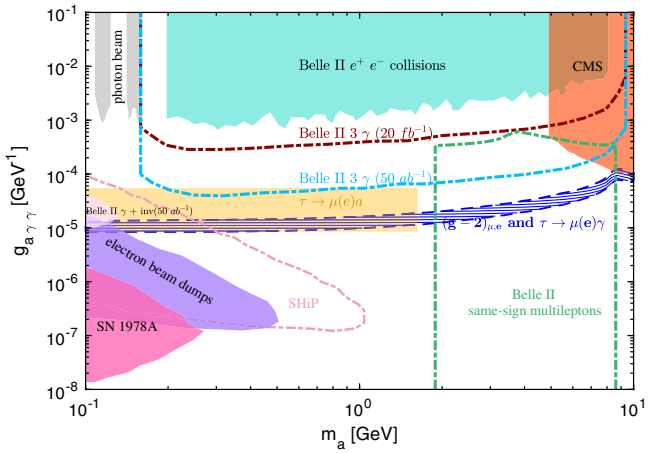

FIG. 4. (Hybrid scenario): Existing and prospected constraints on $(m_a, g_{a\gamma\gamma})$ from various experiments as marked in the plot. The allowed parameter space for $(g-2)_\mu$ and $(g-2)_e$ within the 2σ error has been displayed in the blue slashed area in the center of the figure, which also satisfies constraints from $\tau \to \mu\gamma$ and $\tau \to e\gamma$ processes. The other colored regions are excluded from other experiments. In particular, the yellow shaded region is excluded by $\Gamma_\tau(\text{LFV}) < \Delta\Gamma_\tau$. Thus, the surviving parameter space corresponds to the blue-centered regime labeled as "$(g-2)_{\mu,e}$ and $\tau \to \mu(e)\gamma$" not overlapped with other filled regions with labels of experiments, in color. More details on experimental limits and derived ALP phenomenological trends are referred to as in the text.

[7] Actually, the constraints from both $\tau \to \mu\gamma$ and $\tau \to e\gamma$ require $\cos\theta_{13}\cos\theta_{23} \sim 0$. So we have two cases: (i) $\theta_{13} \sim \pi/2$ and θ_{23} is arbitrary; (ii) $\theta_{23} \sim \pi/2$ and θ_{13} is arbitrary. In the present analysis, we have adopted the second case, since in the allowed range of f_a [Eq. (49)], Δa_e is necessarily too small irrespective to the size of θ_{13} [See the discussions below Eq. (49)]. Therefore, fixing such a potentially free θ_{13} to a specialized value $\sim\pi/2$, as in the first option above, seems to be unnatural, so we have discarded this case.

TABLE III. The allowed parameter region for m_a, f_a, and θ_{23}.

Multilepton constraint	m_a (GeV)	f_a (GeV)	θ_{23}
Not included	$\simeq$(1.7–10)	$\simeq$(12.8–67.9)	$\simeq$(1.42–1.55)
Included	$\simeq$(1.67–1.88), (8.58–10)	$\simeq$(41.0–67.9), (12.8–24.3)	$\simeq$(1.54–1.55), (1.42–1.47)

unconstrained θ_{13} will not affect the surviving parameter space, because θ_{13} is always combined with $\cos\theta_{23} \sim 0$ in the relevant coupling form, as clearly seen from Eq. (47).

(iii) The $\tau \to \mu a$ and $\tau \to e a$ limits give the lower bound on m_a, as in the case of the muon and electron scenarios. $\Gamma(\tau \to \mu a)$ and $\Gamma(\tau \to e a)$ are always predicted to be too large in the present model, so that the whole on-shell ALP process can also be excluded by a general constraint: $\Gamma_\tau(\mathrm{LFV}) < \Delta\Gamma_\tau$, where $\Gamma_\tau(\mathrm{LFV})$ is the partial τ decay width to which the LFV τ decay contributes, and $\Delta\Gamma_\tau$ is the 1 sigma error in measuring the total τ decay width, $\Delta\Gamma_\tau \simeq 3.9 \times 10^{-15}$ GeV [79]. The excluded mass range is shown in the yellow region in Fig. 4.

(iv) On the contrary to $\tau \to \mu a$ and $\tau \to e a$, the prospected limits from the Belle II same-sign multileptons signals will be a smoking-gun to probe or exclude the present ALP, which could give the upper bound on m_a. The sensitivity is depicted as the green-dashed hatched region in Fig. 4. The prospected same-sign multileptons signals are quoted from Ref. [78], where the authors only assume $a - \tau - \mu$ coupling ($c_{\mu\tau}$) without the a-photon coupling. In contrast, the present ALP has nonzero ALP-photon coupling, so the constraint on $c_{\mu\tau}$ in Ref. [78] could be milder than what the authors have obtained. Therefore, the green-dashed hatched region in Fig. 4 might merely correspond to the maximal exclusion limit, and the actual allowed space could be wider. Hence, in the high sensitivity region for Belle II, where 100 MeV $\lesssim m_a \lesssim$ 10 GeV, we find two sets of the allowed ALP mass and decay constant f_a, together with the largest allowed range for θ_{23} in Table III.

The corresponding predicted values of $\mathrm{Br}[\tau \to \mu\gamma]$ and $\mathrm{Br}[\tau \to e\gamma]$ are shown in Table IV.

Thus, the present ALP in the hybrid scenario can be probed by $\tau \to \mu\gamma$ and/or $\tau \to e\gamma$, but cannot have sensitivity to $e^+e^- \to 3\gamma$, even with higher statistics (50 ab^{-1}), as seen from Fig. 4. It is also remarkable to notice that the surviving parameter space points to a part of the currently unexplored "loopholes," which cannot be explored even by the upcoming long-lived particle search experiments, such as SHiP, and only the $\tau \to \mu(e)\gamma$ can probe. In the next subsection, we will propose a more definite signal of the present ALP at Belle II, that is the polarization asymmetry in $\tau \to \mu(e)\gamma$, which can be a punchline of this tau-specific ALP with the MFV.

TABLE IV. Predicted branching ratio value for $\tau \to \mu(e)\gamma$ processes.

Multilepton constraint	$\mathrm{Br}[\tau \to \mu\gamma]$	$\mathrm{Br}[\tau \to e\gamma]$
Not included	$(0\text{–}4.4) \times 10^{-8}$	$(0\text{–}6.7) \times 10^{-9}$
Included	$(0\text{–}4.4) \times 10^{-8}$	$(0\text{–}1.5) \times 10^{-9}, (0\text{–}6.7) \times 10^{-9}$

B. Polarization asymmetry in $\ell_i \to \ell_j\gamma$

We first should observe that the present ALP couples to muon and electron, only through their right-handed chiral components, i.e., μ_R and e_R, because the couplings to light charged leptons arise only through the right-handed flavor rotation, as seen from Eqs. (3), (4), and (5). Thus, in the present framework of the MFV, the ALP couplings to light charged leptons significantly break the parity, hence would generate a sizable left-right asymmetry in the charged-lepton sector physics. Note that the chiral gauge interaction of the SM universally predicts predominantly left-handed polarization. In what follows, we shall show that the present ALP indeed predicts a sizable asymmetry in $\tau \to \mu(e)\gamma$, that can be detected as the polarization asymmetry of the final state photon.

Quantification of the polarization asymmetry in $\tau \to \mu(e)\gamma$ can follow straightforwardly from that in $b \to s\gamma$, which has been discussed in the literature [80,81]. Then, the Wilson coefficients (WCs) of dipole operators (C_7 and C_7') play the central role. For the photon polarization in $\ell_i \to \ell_j\gamma$ decay process, we define the relevant WCs, in a manner similar to those for $b \to s\gamma$ [80,81], as follows:

$$\mathcal{L}^{\ell}_{\mathrm{dipole}} = \frac{G_F}{\sqrt{2}}(C_7^{\ell})_{ji}\frac{e}{16\pi^2}m_{\ell_i}(\bar{\ell}_j\sigma^{\mu\nu}P_R\ell_i)F_{\mu\nu} + \frac{G_F}{\sqrt{2}}(C_7'^{\ell})_{ji}\frac{e}{16\pi^2}m_{\ell_i}(\bar{\ell}_j\sigma^{\mu\nu}P_L\ell_i)F_{\mu\nu}, \quad (50)$$

where $\sigma^{\mu\nu} = \frac{i}{2}[\gamma^\mu, \gamma^\nu]$ and $P_{R/L} \equiv (1 \pm \gamma_5)/2$. Here we have ignored terms proportional to the lighter charged lepton mass, $m_{\ell_j}(\ll m_{\ell_i})$. Then the polarization parameter λ_γ can be defined analogously to the $b \to s\gamma$ case [80,81], as

$$\lambda_\gamma = \frac{\mathrm{Re}[(C_7'^{\ell})_{ji}/(C_7^{\ell})_{ji}]^2 + \mathrm{Im}[(C_7'^{\ell})_{ji}/(C_7^{\ell})_{ji}]^2 - 1}{\mathrm{Re}[(C_7'^{\ell})_{ji}/(C_7^{\ell})_{ji}]^2 + \mathrm{Im}[(C_7'^{\ell})_{ji}/(C_7^{\ell})_{ji}]^2 + 1}. \quad (51)$$

The WCs in Eq. (50) include contributions from both the SM and NP, which is the ALP in the present study. For a reference model, we consider the SM with massive Dirac neutrinos (denoted as SMDν). The model contribution for $\tau \to \mu\gamma$ can be estimated, at the leading nontrivial order in expansion with respect to (m_μ/m_τ), as [80]

$$(C_7^\ell)_{\mu\tau}^{\mathrm{SMD}\nu} \approx \frac{1}{2} A_{\mathrm{SMD}\nu}(x_\nu), \tag{52}$$

$$(C_7'^\ell)_{\mu\tau}^{\mathrm{SMD}\nu} \approx \frac{m_\mu}{m_\tau} (C_7^\ell)_{\mu\tau}^{\mathrm{SMD}\nu}, \tag{53}$$

where $x_\nu = m_\nu^2/m_W^2$, m_ν and m_W are masses of an active neutrino and the W boson, respectively. Here we have simply taken the identical mass for all the active neutrinos, and the PMNS matrix to be unity, which, though being not precisely realistic, will not significantly affect the order of magnitude of estimate on the SMDν contribution. In Eq. (52) the loop function $A_{\mathrm{SMD}\nu(x)}$ reads

$$A_{\mathrm{SMD}\nu}(x) = \frac{-8x^3 - 5x^2 + 7x}{12(x-1)^3} + \frac{3x^3 - 2x^2}{2(x-1)^4} \ln x. \tag{54}$$

Then we get the value of SMDν contribution on the WCs:

$$(C_7^\ell)_{\mu\tau}^{\mathrm{SMD}\nu} \approx -4.51 \times 10^{-27}, \tag{55}$$

$$(C_7'^\ell)_{\mu\tau}^{\mathrm{SMD}\nu} \approx -2.68 \times 10^{-28}. \tag{56}$$

Obviously, $|(C_7^\ell)_{\mu\tau}^{\mathrm{SMD}\nu}| \gg |(C_7'^\ell)_{\mu\tau}^{\mathrm{SMD}\nu}|$ because $m_\mu/m_\tau \ll 1$, which is the consequence of the chirally left-handed gauged weak interaction, as noted above.

As to the NP contribution, the ALP arch and BZ graph amplitudes for $\ell_i \to \ell_j\gamma$ process are given in Refs. [64] and [63], respectively. By translating those formulas back to the Lagrangian operator form, we find the following WCs:

$$(C_7^\ell)_{ji}^{\mathrm{NP}} = -\frac{Q_\ell^{\mathrm{em}}}{2f_a^2} \sum_f \Bigg[-(g_V^\ell)_{jf}(g_V^\ell)_{fi} I_{f,1}^{++} + (g_A^\ell)_{jf}(g_A^\ell)_{fi} I_{f,1}^{+-} - (g_A^\ell)_{jf}(g_V^\ell)_{fi} I_{f,1}^{-+} + (g_V^\ell)_{jf}(g_A^\ell)_{fi} I_{f,1}^{--}$$
$$- \frac{\alpha}{\pi} \frac{1}{(Q_{\ell_i} m_{\ell_i})^2 - (Q_{\ell_j} m_{\ell_j})^2} \{ (Q_{\ell_i} m_{\ell_i} - Q_{\ell_j} m_{\ell_j})(g_A^\ell)_{ji} + (Q_{\ell_i} m_{\ell_i} + Q_{\ell_j} m_{\ell_j})(g_V^\ell)_{ji} \} \frac{(g_A^f)_{ff}}{m_f} f\left(\frac{m_a^2}{m_{\ell_i}^2}, \frac{m_a^2}{m_f^2}\right) \Bigg], \tag{57}$$

$$(C_7'^\ell)_{ji}^{\mathrm{NP}} = -\frac{Q_\ell^{\mathrm{em}}}{2f_a^2} \sum_f \Bigg[-(g_V^\ell)_{jf}(g_V^\ell)_{fi} I_{f,1}^{++} + (g_A^\ell)_{jf}(g_A^\ell)_{fi} I_{f,1}^{+-} + (g_A^\ell)_{jf}(g_V^\ell)_{fi} I_{f,1}^{-+} - (g_V^\ell)_{jf}(g_A^\ell)_{fi} I_{f,1}^{--}$$
$$- \frac{\alpha}{\pi} \frac{1}{(Q_{\ell_i} m_{\ell_i})^2 - (Q_{\ell_j} m_{\ell_j})^2} \{ (Q_{\ell_i} m_{\ell_i} - Q_{\ell_j} m_{\ell_j})(g_A^\ell)_{ji} - (Q_{\ell_i} m_{\ell_i} + Q_{\ell_j} m_{\ell_j})(g_V^\ell)_{ji} \} \frac{(g_A^f)_{ff}}{m_f} f\left(\frac{m_a^2}{m_{\ell_i}^2}, \frac{m_a^2}{m_f^2}\right) \Bigg], \tag{58}$$

where the loop function $f(u, v)$ for the BZ diagram is given in Eq. (23).

Since the present ALP is specifically coupled to μ_R and e_R, as emphasized above, we have $(C_7^\ell)^{\mathrm{NP}} \approx 0$ at the nontrivial-leading order of (m_μ/m_τ). Figure 5 would also help understand this point, where the case of $\tau \to \mu\gamma$ is exemplified. One can see that the nonzero contribution to C_7 necessarily requires the ALP coupling to μ_L (panels

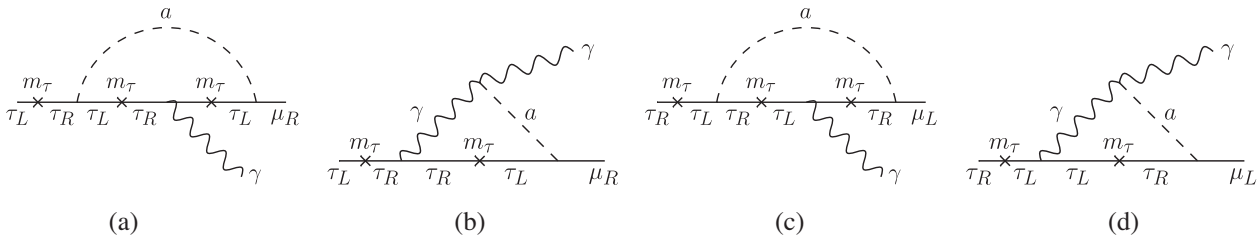

FIG. 5. The arch and BZ diagrams with chirality flips depicted contributing to C_7 and C_7' for $\tau \to \mu\gamma$, at the leading order in expansion with respect to (m_μ/m_τ). To this order, the diagrams (c) and (d) are not generated because of the ALP parity-breaking coupling property for muon. See the text, for more details. (a) $C_7'^\ell$ arch (b) $C_7'^\ell$ BZ (c) C_7^ℓ arch: absent at the leading order (d) C_7^ℓ BZ: absent at the leading order.

(c) and (d) in Fig. 5), which is forbidden at the leading order without suppression by extra chirality flip with m_μ. On the other hand, the C_7' does not yield the chirality flip of muon, as seen from the panel (a) and (b) in Fig. 5. A similar argument is applicable to the case of $\tau \to e\gamma$.

Thus, the present ALP with the MFV and the maximal parity violation predicts

$$|(C_7'^{\ell})^{\rm NP}| \gg |(C_7^{\ell})^{\rm NP}|, \tag{59}$$

in sharp contrast to the SMDν prediction where $|(C_7'^{\ell})^{\rm SM}| \ll |(C_7^{\ell})^{\rm SM}|$, as noted above. We have found that the ALP contributions to the WCs are much greater than the SM contribution: $(C_7'^{\ell})^{\rm NP} = \mathcal{O}(10^{-13}$–$10^{-12})$ in the surviving mass and f_a ranges, see Table III. Thereby, we find a punchline of the present ALP in the polarization asymmetry of Eq. (51):

$$\lambda_\gamma \approx 1, \tag{60}$$

which shows the polarization trend completely opposite to the SMDν's one with $\lambda_\gamma^{\rm SM} \approx -1$.

C. Discrimination from other LFV NP candidates in light of Belle II

In this subsection, we compare phenomenological predictions from the present ALP to those from other LFV NP candidates with the same preferable mass scale as in Eq. (III), within the prospected Belle II reach. Those NP include a light LFV Z' as in Ref. [82], and another type of flavorful ALP, as in Ref. [83].[8]

(i) In Ref. [82], the light Z' predominantly couples to muon and tau lepton. In their work, the preferred Z' mass range consistent with the 2σ deviation range for $(g-2)_\mu$ has been found as $M_{Z'} \simeq 2$–900 MeV, which is promising to be probed at Belle II. Our MFV ALP would be a counter-candidate to this type of Z' in the high mass region in Belle II reach, both of which is accessible at the Belle II through similar LFV signals, as well as accounts for the current deviation in $(g-2)_\mu$. Of crucial is to notice, however, that our ALP can be clearly distinguished from Z' by the punchline, λ_γ, i.e., the polarization asymmetries of $\tau \to \mu\gamma$ and $\tau \to e\gamma$ processes. As we discussed in the last section, the $L-R$ symmetry is significantly and maximally broken by the right-handed rotation due to the MFV criterion, and highly polarized to right-handed, as evident from Eq. (60). In contrast, the LFV Z' is vertorlikely coupled to tau lepton and muon, so no $L-R$ asymmetry is created there. Thus the λ_γ in $\tau \to \mu(e)\gamma$ is the definite discriminator of the present MFV ALP from the light LFV Z'.

(ii) Second, in a recent paper [83], the authors focus on a light ALP having a high enough detection sensitivity at Belle II, through LFV and multilepton signals. Two parallel benchmark scenarios have been investigated in [83], where c_{ee} and $c_{e\tau}$ or $c_{\mu\mu}$ and $c_{\mu\tau}$ are turned on, respectively. There are two possible discriminators to tell the present MFV ALP from theirs. One is λ_γ, because the flavor couplings in their setup are totally independent with each other, not constrained by the MFV, so the parity violation is parametric, therefore no definite value of λ_γ has been predicted in [83]. In contrast, the present MFV ALP is definitely right-handed specific for muon and electron, where the parity is broken only by the right-handed rotation in the framework of the MFV, as emphasized in the previous section. The other discriminator is the trilepton signal where tau decays into three charged leptons. Since the ALP in [83] keeps the flavor-diagonal couplings to muon and electron, the trilepton process is possible to take place. In contrast, the present ALP is tau-specific, and has no flavor-diagonal coupling to muon and electron, as seen from Eq. (47), so the trilepton signals are not produced.

VI. SUMMARY AND DISCUSSION

In summary, we have discussed flavor-physics probes of an intrinsically flavorful ALP (MFV-ALP), with particular focus on a third-generation specific scenario, which generates the tau-lepton LFV processes, to be tested at the Belle II experiment. The ALP is assumed to be tau-philic on the base where the PQ-like charge is defined, inspired by some folklore; "*the third-generation is special*", and is allowed to also couple to muon and electron by the intrinsic MFV arising from the right-handed flavor rotation within the SM. Thus, the ALP couplings to muon and electron are right-handed specific.

We first employed two simplified and separated limits: the electron scenario (Sec. IV A) and muon scenario (Sec. IV B), as in Table II. We found that those scenarios are highly constrained by existing experimental limits from the LFV processes, in particular, $\tau \to e(\mu)\gamma$, and electron or muon $g-2$, so that the mixing angle θ_{13} or θ_{23} is required to extremely be close to $\pi/2$. This implies the preference of

[8] Another Belle II-target NP, which has the potential to explain two $(g-2)$s for light charged leptons, would involve a light dark photon (A') with a mass range similar to the present ALP's, as discussed in Ref. [84] (300 MeV $\lesssim m_{A'} \lesssim$ 1 GeV). This dark photon does not have LFV couplings, so the radiative tau-LFV signals as well as those polarization asymmetries (λ_γ) are the definite discriminators for the present ALP compared to the light dark photon. Furthermore, the light dark photon tends to favor about 2σ deviation for the (negatively pulled) old $\Delta a_e|_{\rm old}$ in Eq. (17), while the present ALP favors the positive value of Δa_e. Hence future experiments on determining the sign of Δa_e can also distinguish the two particles.

a mu or electron-tau flipped feature in the mass eigenbasis when coupled to the ALP.

We then explored a hybrid scenario combining the two separated scenarios by turning on both θ_{13} and θ_{23}. A fully viable parameter space on the ALP mass-photon coupling plane was found. See Fig. 4. The ALP mass is limited in a range, $\sim(1.7\text{–}10)$ GeV and the ALP decay constant f_a is constrained to be $\sim(12.8\text{–}67.9)$ GeV [Eq. (III)], if the same-sign multilepton signals constraint is disregarded. Remarkably, this ALP can be probed only by measurement of $\tau \to \mu\gamma$ and/or $\tau \to e\gamma$ at Belle II.

We find that the same-sign multilepton signal at Belle II is a smoking-gun to probe the present ALP and the polarization asymmetry in $\tau \to \mu\gamma$ and/or $\tau \to e\gamma$ is a punchline, which is definitely predicted to prefer the right-handed polarization due to the MFV [$\lambda_\gamma \approx 1$ Eq. (60)], overwhelming the prediction of the SM with massive Dirac neutrinos having the highly left-handed preference ($\lambda_\gamma^{\rm SM} \approx -1$), in contrast to other light NP candidates which can also be promising to be probed at the Belle II, such as a light LFV Z' and another flavorful ALP.

Several comments and discussions along the future prospect are in order.

(i) The coupling $g_{a\gamma\gamma}$ defined in Eq. (48) includes contribution from both bottom quark loops and tau lepton loops, because in the present study we have focused on a bottom-tau specific ALP. However, even if other quarks are involved in the model by invoking other scenarios, the surviving parameter space (blue-shaded area in the center of Fig. 4) will not substantially be changed, because the quark contributions are not constrained by all the leptonic processes. Other quark contributions will merely increase the value of $g_{a\gamma\gamma}$, without changing the allowed ALP mass and decay constant in Eq. (III). Therefore, the blue shaded area in Fig. 4 will be just pushed upward, if other quarks come into the game. It would then be interesting to see how the surviving parameter space could get into the upper domain filled by the future Belle II prospect reach (at 50 ab^{-1}), which is to be explored elsewhere.

(ii) In cases of electron and muon scenarios, the ALP-quark coupling is necessary to keep $g_{a\gamma\gamma}$ to be sizable, since the ALP-lepton coupling almost vanishes to satisfy experimental constraints.[9] Namely, the ALP-bottom quark coupling would lead to other probes for this third-generation specific scenario. For instance, $b \to d$ and $b \to s$ transitions can be induced dependent on the mixing angles, which would give us some interesting predictions on B flavor physics. We, however, decline to discuss such possibilities, since it is beyond the current scope, and postpone it to elsewhere.[10]

(iii) Possible modeling to underlie the current third-generation specific ALP

(i) The present third-generation-philic ALP can be realized in a way similar to a class of variant QCD axion model with top-specific axion, based on a generic two Higgs doublet model, as discussed in Ref. [87]. In the reference the authors have also argued possible extension to give tau lepton the PQ charge, as well as top quark. As noted above, the bottom quark in the present ALP physics does not play a central role, and may even be replaced with top quark, as far as the lepton flavor physics is concerned. Therefore, the model setup in Ref. [87] would straightforwardly lead to the present tau-specific ALP model. More precisely, to make the ALP mass much larger than a typical QCD axion mass scale, one needs to take the scale of a mass mixing term between two Higgs doublets, which explicitly breaks the PQ symmetry, to be somewhat large, and assume no CP violation in the Higgs sector, and/or the second Higgs boson to be extremely heavy, so that only the ALP is left in the light NP, without extra CP or parity violation.

(ii) The present ALP setup can also be naturally obtained when we consider the Froggatt-Nielsen (FN) mechanism [88].[11] This mechanism can be used for realizing correct hierarchies of Yukawa couplings. In order to obtain appropriate SM fermion masses and CKM structure, Yukawa couplings (Y_u for the up-quark sector; Y_d for the down-quark sector; Y_e for the charged lepton sector) should roughly have the following texture form:

$$Y_u \sim \begin{pmatrix} \lambda^6 & \lambda^5 & \lambda^3 \\ \lambda^5 & \lambda^4 & \lambda^2 \\ \lambda^3 & \lambda^2 & 1 \end{pmatrix}, \quad Y_d \sim \begin{pmatrix} \lambda^6 & \lambda^{5.5} & \lambda^5 \\ \lambda^5 & \lambda^{4.5} & \lambda^4 \\ \lambda^3 & \lambda^{2.5} & \lambda^2 \end{pmatrix},$$
$$Y_e \sim \begin{pmatrix} \lambda^6 & \lambda^5 & \lambda^3 \\ \lambda^{5.5} & \lambda^{4.5} & \lambda^{2.5} \\ \lambda^5 & \lambda^4 & \lambda^2 \end{pmatrix}, \tag{61}$$

[9]Even in the hybrid case, the ALP-bottom quark coupling possibly takes nonzero without conflicting with the experimental constraints on $g_{a\gamma\gamma}$.

[10]The flavor probes of ALPs with generic flavorful coupling are discussed in several articles [52,85,86].

[11]The relationship between the PQ symmetry and a newly introduced global $U(1)$ symmetry for the FN mechanism has been addressed in Refs. [48,49,89–92]. See e.g., Refs. [93–101] for recent attempts.

where $\lambda \simeq 0.22$. This can be easily obtained when we assume an anomalous $U(1)$ charge assigned for SM particles[12] as follows:

$$Q_i:(3,2,0), \quad u^c_{Ri}:(3,2,0), \quad d^c_{Ri}:(3,2.5,2),$$
$$L_i:(3,2.5,2), \quad e^c_{Ri}:(3,2,0), \quad H:0, \quad (62)$$

where Q_i and L_i are quark and lepton doublets, respectively; i denotes the generation index; the upper script c attached on fields stands for the charge conjugation; H denotes the Higgs doublet.

In order to write down the Yukawa couplings, we need to introduce a new scalar field, Θ, which is singlet under SM gauge symmetries and has the anomalous $U(1)$ charge -1. Once Θ acquires the vacuum expectation value like $\langle\Theta\rangle = \lambda\Lambda$, where Λ is some cutoff scale, one can reproduce the hierarchical Yukawa structure in Eq. (61).

In this framework, the ALP-fermion couplings follow the same hierarchies as in Eq. (61), which, therefore, automatically leads to the third-generation-specific ALP. When we assume the ALP to have the anomalous $U(1)$ charge -2, only ALP couplings to bottom and tau lepton arise as $O(1)$, and the other couplings are smaller than $\lambda^2 \sim 0.05$.[13] Thus, the presently analyzed ALP coupling properties can be thought of as an extreme limit of those arising from this FN modeling. We have indeed checked that if we turn on the other ALP-fermion couplings with proper sizes as predicted from the FN mechanism, the results present in the main text will not substantially be changed.[14]

[12]The gauge anomaly associated with this new $U(1)$ gauge symmetry can be canceled by the Green-Schwarz mechanism [102].

ACKNOWLEDGMENTS

We thank Motoi Endo, Syuhei Iguro, and Robert Ziegler for useful comments and discussions. S. M.'s work was supported in part by the National Science Foundation of China (NSFC) under Grants No. 11747308, No. 11975108, No. 12047569 and the Seeds Funding of Jilin University. The work of C. C. has been partially supported by the Tang-Ao Qing (TAQ) honors program in science from the Office of Undergraduate Education and College of Physics in Jilin University.

[13]In the case of nonsupersymmetric models, the ALP-top coupling in this framework is obtained from

$$\left(\frac{\Theta^\dagger}{\Lambda}\right)^2 m_t a(\bar{t}\gamma_5 t) \to \lambda^2 m_t a(\bar{t}\gamma_5 t). \quad (63)$$

In contrast, such terms are absent in supersymmetric models since we cannot use $\Theta^\dagger$ in the superpotential.

[14]Actually, nonzero couplings of Q_e and Q_μ induce a $c_{e\mu}$ coupling in the case of the hybrid scenario, which is severely constrained by LFV processes related to the muon. However, these constraints can be easily avoided by setting $\theta_{13} \sim 0$. Even in this case, the main results of the present paper will not essentially be changed.

[1] R. D. Peccei and H. R. Quinn, Phys. Rev. Lett. **38**, 1440 (1977).
[2] R. D. Peccei and H. R. Quinn, Phys. Rev. D **16**, 1791 (1977).
[3] S. Weinberg, Phys. Rev. Lett. **40**, 223 (1978).
[4] F. Wilczek, Phys. Rev. Lett. **40**, 279 (1978).
[5] I. G. Irastorza and J. Redondo, Prog. Part. Nucl. Phys. **102**, 89 (2018).
[6] L. Di Luzio, M. Giannotti, E. Nardi, and L. Visinelli, Phys. Rep. **870**, 1 (2020).
[7] F. Abudinén *et al.* (Belle-II Collaboration), Phys. Rev. Lett. **125**, 161806 (2020).
[8] B. Abi *et al.* (Muon g-2 Collaboration), Phys. Rev. Lett. **126**, 141801 (2021).
[9] G. W. Bennett *et al.* (Muon g-2 Collaboration), Phys. Rev. D **73**, 072003 (2006).
[10] T. Aoyama, N. Asmussen, M. Benayoun, J. Bijnens, T. Blum, M. Bruno, I. Caprini, C. M. Carloni Calame, M. Cè, G. Colangelo *et al.*, Phys. Rep. **887**, 1 (2020).
[11] T. Aoyama, M. Hayakawa, T. Kinoshita, and M. Nio, Phys. Rev. Lett. **109**, 111808 (2012).
[12] T. Aoyama, T. Kinoshita, and M. Nio, Atoms **7**, 28 (2019).
[13] A. Czarnecki, W. J. Marciano, and A. Vainshtein, Phys. Rev. D **67**, 073006 (2003); **73**, 119901(E) (2006).
[14] C. Gnendiger, D. Stöckinger, and H. Stöckinger-Kim, Phys. Rev. D **88**, 053005 (2013).
[15] M. Davier, A. Hoecker, B. Malaescu, and Z. Zhang, Eur. Phys. J. C **77**, 827 (2017).
[16] A. Keshavarzi, D. Nomura, and T. Teubner, Phys. Rev. D **97**, 114025 (2018).
[17] G. Colangelo, M. Hoferichter, and P. Stoffer, J. High Energy Phys. 02 (2019) 006.
[18] M. Hoferichter, B. L. Hoid, and B. Kubis, J. High Energy Phys. 08 (2019) 137.
[19] M. Davier, A. Hoecker, B. Malaescu, and Z. Zhang, Eur. Phys. J. C **80**, 241 (2020); **80**, 410(E) (2020).

[20] A. Keshavarzi, D. Nomura, and T. Teubner, Phys. Rev. D **101**, 014029 (2020).
[21] A. Kurz, T. Liu, P. Marquard, and M. Steinhauser, Phys. Lett. B **734**, 144 (2014).
[22] K. Melnikov and A. Vainshtein, Phys. Rev. D **70**, 113006 (2004).
[23] P. Masjuan and P. Sanchez-Puertas, Phys. Rev. D **95**, 054026 (2017).
[24] G. Colangelo, M. Hoferichter, M. Procura, and P. Stoffer, J. High Energy Phys. 04 (2017) 161.
[25] M. Hoferichter, B. L. Hoid, B. Kubis, S. Leupold, and S. P. Schneider, J. High Energy Phys. 10 (2018) 141.
[26] A. Gérardin, H. B. Meyer, and A. Nyffeler, Phys. Rev. D **100**, 034520 (2019).
[27] J. Bijnens, N. Hermansson-Truedsson, and A. Rodríguez-Sánchez, Phys. Lett. B **798**, 134994 (2019).
[28] G. Colangelo, F. Hagelstein, M. Hoferichter, L. Laub, and P. Stoffer, J. High Energy Phys. 03 (2020) 101.
[29] T. Blum, N. Christ, M. Hayakawa, T. Izubuchi, L. Jin, C. Jung, and C. Lehner, Phys. Rev. Lett. **124**, 132002 (2020).
[30] G. Colangelo, M. Hoferichter, A. Nyffeler, M. Passera, and P. Stoffer, Phys. Lett. B **735**, 90 (2014).
[31] M. Davier, A. Hoecker, B. Malaescu, and Z. Zhang, Eur. Phys. J. C **71**, 1515 (2011); **72**, 1874(E) (2012).
[32] M. Bauer, M. Neubert, S. Renner, M. Schnubel, and A. Thamm, Phys. Rev. Lett. **124**, 211803 (2020).
[33] S. F. Ge, X. D. Ma, and P. Pasquini, Eur. Phys. J. C **81**, 787 (2021).
[34] W. Y. Keung, D. Marfatia, and P. Y. Tseng, Lett. High Energy Phys. **2021**, 209 (2021).
[35] S. M. Barr and A. Zee, Phys. Rev. Lett. **65**, 21 (1990); **65**, 2920(E) (1990).
[36] J. Jaeckel and M. Spannowsky, Phys. Lett. B **753**, 482 (2016).
[37] M. Bauer, M. Neubert, and A. Thamm, J. High Energy Phys. 12 (2017) 044.
[38] M. J. Dolan, T. Ferber, C. Hearty, F. Kahlhoefer, and K. Schmidt-Hoberg, J. High Energy Phys. 12 (2017) 094; 03 (2021) 190(E).
[39] J. Beacham, C. Burrage, D. Curtin, A. De Roeck, J. Evans, J. L. Feng, C. Gatto, S. Gninenko, A. Hartin, I. Irastorza *et al.*, J. Phys. G **47**, 010501 (2020).
[40] B. Döbrich, J. Jaeckel, and T. Spadaro, J. High Energy Phys. 05 (2019) 213; 10 (2020) 046(E).
[41] M. A. Buen-Abad, J. Fan, M. Reece, and C. Sun, J. High Energy Phys. 09 (2021) 101.
[42] C. Dohmen *et al.* (SINDRUM II Collaboration), Phys. Lett. B **317**, 631 (1993).
[43] W. Honecker *et al.* (SINDRUM II Collaboration), Phys. Rev. Lett. **76**, 200 (1996).
[44] W. H. Bertl *et al.* (SINDRUM II Collaboration), Eur. Phys. J. C **47**, 337 (2006).
[45] M. Endo, S. Iguro, and T. Kitahara, J. High Energy Phys. 06 (2020) 040.
[46] P. H. Frampton, arXiv:hep-ph/9409331.
[47] P. H. Frampton, arXiv:hep-ph/9507351.
[48] A. Davidson and K. C. Wali, Phys. Rev. Lett. **48**, 11 (1982).
[49] F. Wilczek, Phys. Rev. Lett. **49**, 1549 (1982).
[50] Z. G. Berezhiani and M. Y. Khlopov, Z. Phys. C **49**, 73 (1991).
[51] J. Heeck and W. Rodejohann, Phys. Lett. B **776**, 385 (2018).
[52] L. Calibbi, D. Redigolo, R. Ziegler, and J. Zupan, J. High Energy Phys. 09 (2021) 173.
[53] G. Haghighat and M. Mohammadi Najafabadi, arXiv:2106.00505.
[54] S. Alekhin, W. Altmannshofer, T. Asaka, B. Batell, F. Bezrukov, K. Bondarenko, A. Boyarsky, K. Y. Choi, C. Corral, N. Craig *et al.*, Rep. Prog. Phys. **79**, 124201 (2016).
[55] J. L. Feng, I. Galon, F. Kling, and S. Trojanowski, Phys. Rev. D **98**, 055021 (2018).
[56] E. Kou *et al.* (Belle-II Collaboration), Prog. Theor. Exp. Phys. **2019**, 123C01 (2019); **2020**, 029201(E) (2020).
[57] H. Ishida, S. Matsuzaki, and Y. Shigekami, Phys. Rev. D **103**, 095022 (2021).
[58] N. Cabibbo, Phys. Rev. Lett. **10**, 531 (1963).
[59] M. Kobayashi and T. Maskawa, Prog. Theor. Phys. **49**, 652 (1973).
[60] B. Pontecorvo, Zh. Eksp. Teor. Fiz. **34**, 247 (1957).
[61] Z. Maki, M. Nakagawa, and S. Sakata, Prog. Theor. Phys. **28**, 870 (1962).
[62] M. Bauer, M. Neubert, S. Renner, M. Schnubel, and A. Thamm, J. High Energy Phys. 04 (2021) 063.
[63] C. Cornella, P. Paradisi, and O. Sumensari, J. High Energy Phys. 01 (2020) 158.
[64] M. Lindner, M. Platscher, and F. S. Queiroz, Phys. Rep. **731**, 1 (2018).
[65] D. Chang, W. F. Chang, C. H. Chou, and W. Y. Keung, Phys. Rev. D **63**, 091301 (2001).
[66] D. Buttazzo, P. Panci, D. Teresi, and R. Ziegler, Phys. Lett. B **817**, 136310 (2021).
[67] L. Morel, Z. Yao, P. Cladé, and S. Guellati-Khélifa, Nature (London) **588**, 61 (2020).
[68] D. Hanneke, S. Fogwell, and G. Gabrielse, Phys. Rev. Lett. **100**, 120801 (2008).
[69] R. Garcia-Martin, R. Kaminski, and J. R. Pelaez, Int. J. Mod. Phys. A **24**, 590 (2009).
[70] D. Hanneke, S. F. Hoogerheide, and G. Gabrielse, Phys. Rev. A **83**, 052122 (2011).
[71] K. Hayasaka, K. Inami, Y. Miyazaki, K. Arinstein, V. Aulchenko, T. Aushev, A. M. Bakich, A. Bay, K. Belous, V. Bhardwaj *et al.*, Phys. Lett. B **687**, 139 (2010).
[72] A. M. Baldini *et al.* (MEG II Collaboration), Eur. Phys. J. C **78**, 380 (2018).
[73] H. Albrecht *et al.* (ARGUS Collaboration), Z. Phys. C **68**, 25 (1995).
[74] D. Aloni, C. Fanelli, Y. Soreq, and M. Williams, Phys. Rev. Lett. **123**, 071801 (2019).
[75] A. M. Sirunyan *et al.* (CMS Collaboration), Phys. Lett. B **797**, 134826 (2019).
[76] J. Jaeckel, P. C. Malta, and J. Redondo, Phys. Rev. D **98**, 055032 (2018).
[77] B. Döbrich, J. Jaeckel, F. Kahlhoefer, A. Ringwald, and K. Schmidt-Hoberg, J. High Energy Phys. 02 (2016) 018.
[78] S. Iguro, Y. Omura, and M. Takeuchi, J. High Energy Phys. 09 (2020) 144.
[79] P. A. Zyla *et al.* (Particle Data Group), Prog. Theor. Exp. Phys. **2020**, 083C01 (2020).

[80] E. Kou, C. D. Lü, and F. S. Yu, J. High Energy Phys. 12 (2013) 102.
[81] N. Haba, H. Ishida, T. Nakaya, Y. Shimizu, and R. Takahashi, J. High Energy Phys. 03 (2015) 160.
[82] J. Heeck, Phys. Lett. B **758**, 101 (2016).
[83] K. Cheung, A. Soffer, Z. S. Wang, and Y. H. Wu, J. High Energy Phys. 11 (2021) 218.
[84] G. Mohlabeng, Phys. Rev. D **99**, 115001 (2019).
[85] J. Martin Camalich, M. Pospelov, P. N. H. Vuong, R. Ziegler, and J. Zupan, Phys. Rev. D **102**, 015023 (2020).
[86] M. Bauer, M. Neubert, S. Renner, M. Schnubel, and A. Thamm, arXiv:2110.10698.
[87] C. W. Chiang, H. Fukuda, M. Takeuchi, and T. T. Yanagida, J. High Energy Phys. 11 (2015) 057.
[88] C. D. Froggatt and H. B. Nielsen, Nucl. Phys. **B147**, 277 (1979).
[89] D. B. Reiss, Phys. Lett. **115B**, 217 (1982).
[90] A. Davidson, V. P. Nair, and K. C. Wali, Phys. Rev. D **29**, 1504 (1984).
[91] Z. G. Berezhiani and M. Y. Khlopov, Sov. J. Nucl. Phys. **51**, 739 (1990).
[92] Z. G. Berezhiani and M. Y. Khlopov, Sov. J. Nucl. Phys. **51**, 935 (1990).
[93] Y. Ema, K. Hamaguchi, T. Moroi, and K. Nakayama, J. High Energy Phys. 01 (2017) 096.
[94] L. Calibbi, F. Goertz, D. Redigolo, R. Ziegler, and J. Zupan, Phys. Rev. D **95**, 095009 (2017).
[95] F. Arias-Aragon and L. Merlo, J. High Energy Phys. 10 (2017) 168; 11 (2019) 152(E).
[96] F. Björkeroth, E. J. Chun, and S. F. King, Phys. Lett. B **777**, 428 (2018).
[97] M. Linster and R. Ziegler, J. High Energy Phys. 08 (2018) 058.
[98] F. Björkeroth, E. J. Chun, and S. F. King, J. High Energy Phys. 08 (2018) 117.
[99] Q. Bonnefoy, E. Dudas, and S. Pokorski, J. High Energy Phys. 01 (2020) 191.
[100] C. D. Carone and M. Merchand, Phys. Rev. D **101**, 115032 (2020).
[101] L. M. G. de la Vega, N. Nath, S. Nellen, and E. Peinado, Eur. Phys. J. C **81**, 608 (2021).
[102] M. B. Green and J. H. Schwarz, Phys. Lett. **149B**, 117 (1984).